

**South Dakota State University**  
**Open PRAIRIE: Open Public Research Access Institutional  
Repository and Information Exchange**

---

GSCE Faculty Publications

Geospatial Sciences Center of Excellence (GSCE)

---

6-2014

# Interannual Variation in Biomass Burning and Fire Seasonality Derived from Geostationary Satellite Data Across the Contiguous United States from 1995 to 2011

Xiaoyang Zhang

*South Dakota State University, [xiaoyang.zhang@sdstate.edu](mailto:xiaoyang.zhang@sdstate.edu)*


Shobha Kondragunta

*NOAA/NESDIS/Center for Satellite Applications and Research*

David Roy

*[david.roy@sdstate.edu](mailto:david.roy@sdstate.edu)*

Follow this and additional works at: [http://openprairie.sdstate.edu/gsce\\_pubs](http://openprairie.sdstate.edu/gsce_pubs)

 Part of the [Climate Commons](#), [Environmental Sciences Commons](#), [Geographic Information Sciences Commons](#), and the [Spatial Science Commons](#)

---

## Recommended Citation

Zhang, Xiaoyang; Kondragunta, Shobha; and Roy, David, "Interannual Variation in Biomass Burning and Fire Seasonality Derived from Geostationary Satellite Data Across the Contiguous United States from 1995 to 2011" (2014). *GSCE Faculty Publications*. Paper 6.

[http://openprairie.sdstate.edu/gsce\\_pubs/6](http://openprairie.sdstate.edu/gsce_pubs/6)

This Article is brought to you for free and open access by the Geospatial Sciences Center of Excellence (GSCE) at Open PRAIRIE: Open Public Research Access Institutional Repository and Information Exchange. It has been accepted for inclusion in GSCE Faculty Publications by an authorized administrator of Open PRAIRIE: Open Public Research Access Institutional Repository and Information Exchange. For more information, please contact [michael.biondo@sdstate.edu](mailto:michael.biondo@sdstate.edu).

## RESEARCH ARTICLE

10.1002/2013JG002518

## Key Points:

- Fire season shifts early with a rate of 1.5–5 d/yr
- Biomass consumed has increased by 2.87 Tg/yr
- Fire seasons are controlled by climate and agricultural practices

## Correspondence to:

X. Zhang,  
xiaoyang.zhang@sdstate.edu

## Citation:

Zhang, X., S. Kondragunta, and D. P. Roy (2014), Interannual variation in biomass burning and fire seasonality derived from geostationary satellite data across the contiguous United States from 1995 to 2011, *J. Geophys. Res. Biogeosci.*, 119, 1147–1162, doi:10.1002/2013JG002518.

Received 24 SEP 2013

Accepted 16 MAY 2014

Accepted article online 22 MAY 2014

Published online 13 JUN 2014

## Interannual variation in biomass burning and fire seasonality derived from geostationary satellite data across the contiguous United States from 1995 to 2011

Xiaoyang Zhang<sup>1</sup>, Shobha Kondragunta<sup>2</sup>, and David P. Roy<sup>1</sup>

<sup>1</sup>Geospatial Sciences Center of Excellence, South Dakota State University, Brookings, South Dakota, USA, <sup>2</sup>NOAA/NESDIS/Center for Satellite Applications and Research, College Park, Maryland, USA

**Abstract** Wildfires exhibit a strong seasonality that is driven by climatic factors and human activities. Although the fire seasonality is commonly determined using burned area and fire frequency, it could also be quantified using biomass consumption estimates that directly represent biomass loss (a combination of the area burned and the fuel loading). Therefore, in this study a data set of long-term biomass consumed was derived from geostationary satellite data to explore the interannual variation in the fire seasonality and the possible impacts of climate change and land management practices across the Contiguous United States (CONUS). Specifically, daily biomass consumed data were derived using the fire radiative power retrieved from Geostationary Operational Environmental Satellites series with a pixel size of 4–10 km from 1995 to 2011. Annual fire seasonality metrics including the fire season duration, the timing of the start, peak, and end of the fire season, and interannual variation and trends were derived from the 17 year biomass consumed record. These metrics were associated with climatic factors to examine drivers and mediators of fire seasonality. The results indicate that biomass consumed significantly increased at a rate of 2.87 Tg/yr; however, the derived fire season duration exhibited a shortening trend in various states over the western CONUS and no significant trend in most other regions. This suggests that the frequency of extreme fire events has increased, which is perhaps associated with an observed increase of extreme weather conditions. Further, both the start and the end of the fire season exhibited an early shift (1.5–5 d/yr) in various eastern states although a late shift occurred in Arizona and Oregon. The interannual variation and trend in the fire seasonality was more strongly related to temperature in the western CONUS and to precipitation in the southeast. The Palmer Drought Severity Index was found to effectively reflect interannual variations in total biomass consumed although it was poorly correlated to the fire seasonality metrics. The results indicate that across the CONUS, the spatial patterns of the start, peak, and end of the fire season shift regularly in various regions in response to latitudinal gradients of temperature variation.

### 1. Introduction

Wildfires have a significant influence on ecosystem structure and function, trace gas emissions, carbon cycle, air quality, energy feedbacks to the climate system, regional socioeconomic conditions, and future land use planning [Chapin *et al.*, 2003; Randerson *et al.*, 2006; Balshi *et al.*, 2007, 2009]. These influences may vary greatly with the seasonal occurrence and activity of wildfires [Russell-Smith *et al.*, 2009; Le Page *et al.*, 2010a; Ge *et al.*, 2013]. The principal characteristics of fires in a region are often referred to as the fire regime, usually characterized in terms of the seasonality, frequency, spread patterns, intensity, fuel consumption, and severity of fires [Bond and Keeley, 2005; Gill, 1975]. As the climate becomes warmer over a long time scale, the fire season is likely to be shifted and altered with more widespread and frequent fires [Intergovernmental Panel on Climate Change (IPCC), 2007], and in the United States, the fire season is expected to lengthen with earlier and later annual start and end dates respectively [Westerling *et al.*, 2006]. This could lead to a change of both spatial fire patterns and fire regimes [Kasischke *et al.*, 1995; Weber and Flannigan, 1997; Flannigan *et al.*, 2000]. How fire regimes will change in the face of shifting human populations, alterations in land use practices, and the impacts of climate change remains unclear [Chuvienco *et al.*, 2008; Bowman *et al.*, 2009].

Determination of the fire seasonality at regional and global scales is important for characterizing fire regimes, variation in biomass burning emissions, and fire climate impacts [Pausas and Keeley, 2009; Le Page *et al.*, 2010b].

Several climate-related indices have been developed to describe potential fire seasonality. Specifically, the Fire Potential Index has been designed to quantify a season that is susceptible to fire ignition; it is derived by integrating meteorological factors (temperature and relative humidity), fuel maps, and long-term normalized difference vegetation index variations derived from the advanced very high resolution radiometer or the MODIS (Moderate Resolution Imaging Spectroradiometer) satellite systems [Burgan *et al.*, 1998; Huesca *et al.*, 2009]. The Chandler Burning Index provides an index of fire susceptibility that is based on temperature and relative humidity, and has been used to indicate eco-climatic fire seasonality globally [Chandler *et al.*, 1983; Le Page *et al.*, 2010b].

Fire seasonality has also been estimated using various fire regime attributes including the fire frequency, burned area, fire intensity, and fire severity [Weber and Flannigan, 1997]. Historical fire inventories of burned area and fire frequency are commonly used for monitoring wildfire properties. For example, time series of historical burned area at different time scales [Riaño *et al.*, 2007; Pereira *et al.*, 2011] have been used to quantify the fire season length and the timing of the start of the fire season [Taylor and Skinner, 2003; Lee *et al.*, 2006; Westerling *et al.*, 2006], and the reported time between the first wildfire discovery date and the last wildfire control date has been applied to derive the long-term variation in the fire season [Westerling *et al.*, 2006].

Satellite observations available over the last several decades provide synoptic repeat coverage observations with fire monitoring capabilities [Roy *et al.*, 2013]. The frequency and seasonality of fire can be derived in a demonstrably reliable manner from satellite data, usually as summary statistics of satellite-derived burned area maps or active fire counts [Chuvieco *et al.*, 2008; Csiszar *et al.*, 2005; Giglio *et al.*, 2006; Chen *et al.*, 2011; Magi *et al.*, 2012]. The fire radiative power (FRP) can be directly retrieved from middle-infrared wavelength remotely sensed data at the locations of active fire detections. The FRP is directly proportional to the rate of fuel consumption and so is a function of the fuel loading, the combustion efficiency, and the subpixel burned area [Wooster *et al.*, 2003]. As a result, the time integration of FRP over the duration of the fire, termed the fire radiative energy (FRE), has been used to estimate Biomass Consumed in Dry Mass (BCDM) for Africa [Ellicott *et al.*, 2009] and globally [Kaiser *et al.*, 2009, 2012; Zhang *et al.*, 2012]. The temporal integration of FRP to FRE is sensitive to the satellite sampling and cloud and smoke obscuration, as fires may not be burning at the time of satellite overpass, or may be sensed when the fire is not fully burning, and because the fire behavior can fluctuate rapidly in space and time [Smith and Wooster, 2005; Kumar *et al.*, 2011; Boschetti and Roy, 2009]. These factors limit particularly the utility of polar-orbiting satellites that overpass only several times per day at the equator and midlatitudes. Geostationary systems sense the Earth every 15 to 30 min and so are less sensitive to these issues. For example, satellite FRP-derived fuel consumption amounts for African savanna grasslands have been shown to be in broad agreement with literature values [Roberts *et al.*, 2009]. Therefore, it is advantageous to use high temporal frequency geostationary biomass consumed estimates to examine the fire seasonality because this quantity directly represents biomass loss (a combination of the burned area and the fuel loading) and can be generated at sufficiently high temporal frequency to be less sensitive to cloud and smoke obscuration.

This study investigated the fire seasonality and its interannual variation by analyzing time series of daily BCDM across the contiguous United States (CONUS) from 1995 to 2011. A 17 year BCDM data set was first generated from FRP observations retrieved from Geostationary Operation Environmental Satellites (GOES). The time series of BCDM was then used to estimate annual fire seasonality metrics including the fire season duration, and the timing of the start, peak, and end of the fire season. The interannual variation and trend in the fire seasonality during the past 17 years were further analyzed. Finally, the impact of climate change on fire season changes was investigated.

## 2. Methods

### 2.1. GOES Fire Radiative Power Data and Biomass Combusted Estimation

The Wildfire Automated Biomass Burning Algorithm (WF\_ABBA) V65 fire product [Prins *et al.*, 1998; Weaver *et al.*, 2004] was used. Although FRP is theoretically a function of fire size and fire temperature that can be derived for subpixels using a bispectral approach [Peterson *et al.*, 2013a, 2013b], WF\_ABBA derives FRP using the approach established by Wooster *et al.* [2003], which is based on the difference of middle-infrared spectral radiances between a fire pixel and ambient background pixels. WF\_ABBA FRP has a temporal

resolution of 30 min and a spatial resolution of 4 to 10 km varying across the CONUS with the GOES-E imager view zenith angle. The 30 min product is available from 1995 to 2011 but the data for 1996 were discarded because of noise issues observed for this year. The WF\_ABBA V65 fire product provides the time of fire detection, the fire location latitude and longitude, an instantaneous estimate of FRP, a Global Land Cover Characterization (GLCC) ecosystem type ([http://edc2.usgs.gov/glcc/globdoc2\\_0.php](http://edc2.usgs.gov/glcc/globdoc2_0.php)), and a quality flag. The product has only been available since GOES 8 became operational in 1995. This is because the imager onboard the GOES 8 and later satellites offers higher temporal and spatial resolution (4 km at nadir), greater radiometric sensitivity, and improved navigation, compared to the visible infrared spin scan radiometer atmospheric sounder onboard the previous GOES 7 [Prins *et al.*, 1998]. Potential imitations of the WF\_ABBA V65 fire product are described in the context of this research in section 4.

The diurnal variation in FRP data for each individual fire pixel was simulated to reconstruct any missed FRP observations in the WF\_ABBA product due to cloud and saturated pixels that were discarded [Zhang *et al.*, 2012]. Briefly, the diurnal pattern was reconstructed by fitting a climatological FRP diurnal pattern to the available fire FRP observations in a given pixel. The climatological FRP diurnal pattern was generated for five CONUS ecosystem types based on good quality FRP from 2002 to 2005. The ecosystems were reclassified from the 96 GLCC ecosystem types provided in WF\_ABBA into forests, savannas, shrublands, grasslands, and croplands. Assuming that the shape of the FRP diurnal pattern is similar to the climatology in a given ecosystem, the magnitude of the reconstructed FRP for an individual fire pixel was controlled by the observed good quality FRP data and the shape was controlled by the climatological FRP [Zhang *et al.*, 2012]. This approach can also replace the saturated fire pixels, but the actual value is possibly underestimated because the fire temperature in such pixels is generally high.

The daily biomass combusted in dry mass was calculated from the simulated diurnal FRP at pixel locations where the WF\_ABBA V65 product detected fire. Wooster [2002] demonstrated a linear relationship between fuel consumption and total emitted fire radiative energy as follows:

$$\text{BCDM} = \text{FRE} \times \beta = \int_{t_1}^{t_2} \text{FRP} dt \times \beta \quad (1)$$

where BCDM is the biomass consumed (kg), FRP is the fire radiative power (MW), FRE is the fire radiative energy (MJ),  $t_1$  and  $t_2$  are the beginning and ending times (s) of biomass burning, and  $\beta$  is biomass combustion rate (kg/MJ). Fires do not necessarily burn for a whole day and instantaneous fires may not be continuously detected by GOES due to the impact of cloud cover, smoke, cool and/or small fires releasing limited fire energy, and other detection factors. Consequently, the fire duration was determined by assuming that the fire could be extended by 2 h prior to and after the instantaneous fire detections if there were more than three fire observations (all quality levels) within a day [Zhang *et al.*, 2011]. Otherwise, the FRPs for less than three fire occurrences were used to stand alone.

The biomass combustion rate ( $\beta$ ) is assumed to be a constant. This is due to the fact that the energy content of dry biomass does not vary considerably across different ecosystems and fuel types [Pooter and Villar, 1997; Chapin *et al.*, 2002] and that the actual heat yield of a fire event is little influenced by environmental factors including slope, fuel arrangement, and wind speed [Whelan, 1995; Scott, 2000]. Because satellite-derived FRE represents all the energy released from fires, the calculation of biomass consumed could include the contribution from dead organic matter at the surface and the soil. The relationship between the amount of biomass burned and FRE has been investigated based on both laboratory and field measurements, and although the fuel types and locations were different, the  $\beta$  variation has been found to be limited. Field-controlled experiments have indicated that the combustion rate is  $0.368 \pm 0.015$  kg/MJ for Miscanthus grass (including woody oak and hickory) with a fuel moisture of 12% [Wooster *et al.*, 2005]. Laboratory-controlled experiments in a combustion chamber have demonstrated that the rate is 0.453 kg/MJ for mixed fuel beds (pine needles, pine branches, fir twigs, fir foliage, live herbaceous, senesced grass, and big sagebrush) with a dead fuel moisture contents of 7.1% ( $\pm 1.3\%$ ) and live moisture content of up to 44.8% [Freeborn *et al.*, 2008]. Because the latter contains a wide range of fuel types and fuel moisture contents, the biomass combustion rate of 0.453 kg/MJ was adopted for this study.

## 2.2. Detection of Fire Seasonality From Daily Biomass Consumed

Daily biomass consumed was computed for each CONUS GOES pixel with a fire detection. Because fire occurrence is episodic, it is impractical to describe the daily variation using a numerical function for a pixel. As

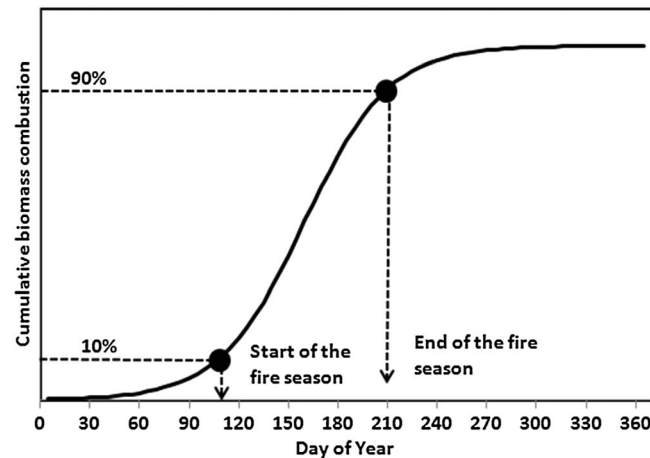


Figure 1. Schematic for determination of the fire seasonality.

daily biomass consumed (kg) calculated from equation (1),  $T$  is the total number of days in a year (365 or 366 for leap years), and  $\gamma$  and  $\delta$  are the shape parameters of the equation defined using the Levenberg-Marquardt method [Press et al., 1997].

Fire season metrics were derived from (2), specifically, the start, peak, end, and duration of the fire season. It was assumed that the start and end of a fire season occurred on the days of the year when  $BCDM_c(t)$  reached 10% and 90% of the total annual biomass consumed, respectively (Figure 1). The peak fire season was calculated by identifying the middle day within a moving 60 day window where the maximum 60 day BCDM occurs during a year. The moving window size was determined by analyzing the minimum fire season duration, which was about 2 months across the CONUS.

### 2.3. Analysis of Spatial and Temporal Variation of Biomass Consumed and Seasonality

Because of the spatiotemporally discrete nature of the biomass consumed, the values from individual GOES pixels were aggregated to a spatial scale of a quarter degree grid, 1° grid, and at state level, respectively. The aggregation was undertaken by taking the arithmetic mean for the fire season metrics and the total for the biomass consumed. Both the spatial pattern and interannual variation in the fire seasonality were examined in grid cells. At the state level, the biomass consumed was stratified based on the forest, savanna, shrubland, grassland, and cropland ecosystem types to investigate the contribution of different ecosystems to biomass consumed. The interannual variation and trend at a state scale were further analyzed using an ordinary least squares (OLS) method that does not consider the effect of serially correlated residuals. Note that the possible autocorrelation in the time series may exaggerate the statistical significance in the trend analysis using OLS [Thejll and Schmith, 2005].

### 2.4. Climate Data and Comparison With Biomass Consumed Seasonality

It has been demonstrated using different methods that climate factors such as the antecedent and current temperature, precipitation, and the degree of drought are important factors in mediating fire [Balshi et al., 2009; Littell et al., 2009]. We recognize that these and other multiple factors may combine in complex ways [Archibald et al., 2009; Westerling et al., 2011], but in this study a simple analysis was conducted to investigate each of these factor independently on the derived BCDM fire season metrics.

Climate data from 1995 to 2011 were acquired from the NOAA National Centers for Environmental Prediction (NCEP) North America Regional Reanalysis (NARR), which have been demonstrated to be effective in investigating fire weather forecasting [Peterson et al., 2010]. The NCEP NARR produces 3-hourly precipitation and temperature data at a spatial resolution of 32 km (approximately 0.25°) [Mesinger et al., 2006], which were aggregated to daily data in this study. In addition, the monthly Palmer Drought Severity Index (PDSI; known operationally as the Palmer Drought Index) was obtained from the NOAA National Climatic Data Center (<http://www1.ncdc.noaa.gov/pub/data/cirs/>) for individual states from 1995 to 2011. The PDSI was originally developed by Palmer [1965] with the intention of measuring the cumulative departure in surface water

an alternative, the cumulative distribution was used to functionalize the daily variation in combusted biomass. After testing several curve fitting models, the sigmoid model was selected to describe the temporal distribution of cumulative biomass consumed as follows:

$$BCDM_c(t) = \frac{BCDM_T}{1 + e^{\delta + \gamma t}} \quad (2)$$

$$BCDM_T = \sum_{t=1}^T BCDM(t) \quad (3)$$

where  $BCDM_c(t)$  is the cumulative biomass consumed (kg) up to day of year  $t$ ,  $BCDM_T$  is the total annual biomass consumed (kg),  $BCDM(t)$  is



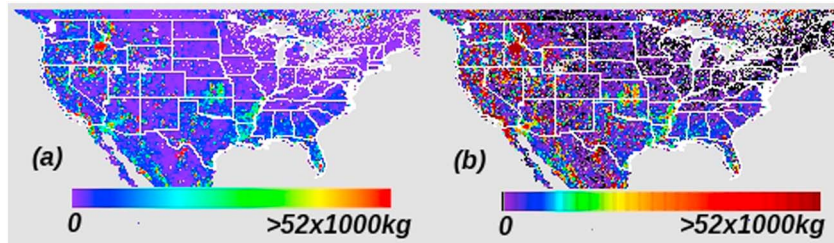


**Figure 2.** (a) Average of annual biomass combusted and (b) standard deviation of annual biomass consumed in a 0.25° grid for 1995–2011.

balance. It incorporates antecedent and current moisture supply (precipitation) and demand (potential evapotranspiration) into a hydrological accounting system to measure the duration and intensity of long-term drought. The intensity of drought during the current month is dependent on the current weather patterns plus the cumulative patterns of previous months [Dai, 2011]. Consequently, positive PDSI values indicate wetter than normal conditions, while negative values suggest levels of drought as follows: normal (0 to -0.5), incipient drought (-0.5 to -1.0), mild drought (-1.0 to -2.0), moderate drought (-2.0 to -3.0), severe drought (-3.0 to -4.0), and extreme drought (< -4.0).

The climate parameters were statistically correlated to the fire seasonality using an ordinary least squares method. Specifically, the means of the start and the end of the fire season in the 17 years were correlated to the means of the temperature, precipitation, and the PDSI derived for the current and the previous month at state scales, respectively. Further, for each state, the 17 annual BCDM estimates were compared with the mean state PDSI. In these analyses, only the significant correlations (*P* value < 0.1) were discussed.

### 3. Results

#### 3.1. Spatial and Temporal Pattern of Biomass Consumed

The annual biomass consumed was computed as equation (3). Figure 2a presents the spatial distribution of the average annual BCDM across the CONUS from 1995 to 2011. On average, fires burned  $52.7 \pm 26.5$  Tg dry biomass per year. As expected, the largest consumption appeared in the western CONUS where fuel loads and burned areas are greater, followed by the southeastern region, and by the Mississippi valley where fires are particularly prevalent [Zhang *et al.*, 2008]. Figure 2b shows the standard deviation of the annual biomass consumed, which reflects the interannual variation in a 0.25° grid cell. The standard deviation was large in high BCDM regions, which closely followed the spatial pattern of long-term average BCDM. The coefficient of variation of these data (cv: standard deviation/mean) was greater than unity in some local areas. The large interannual variation in a given region is mostly attributed to individual extreme fire events. For example, the fire event of 1–20 June 2011 in Arizona (111°W, 34°N to 108°W, 32.5°N) burned 9.25 Tg of dry mass (Figure 3), which accounts for 8.8% of the CONUS BCDM for 2011.

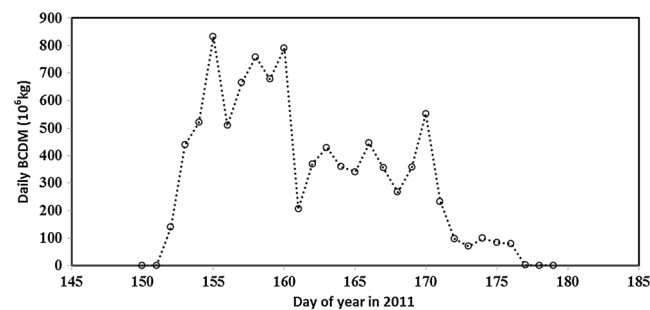


**Figure 3.** Daily development of biomass consumption for an individual fire event that occurred in Arizona (111°W, 34°N to 108°W, 32.5°N) from 1 to 20 June 2011.

The biomass consumed varied greatly by state and ecosystem over the 17 years. The largest biomass burning occurred in the following 10 states: California, Idaho, Texas, Montana, Arizona, Oregon, Kansas, Florida, Arkansas, and Nevada, which account for 67% of total BCDM (Figure 4). On average, the proportion of BCDM is 53.9% in forests (mainly in California, Idaho, Montana, Oregon, and Florida), 11.7% in savannas (mainly in California, Arizona, Colorado, Kansas, and New Mexico), 35.2% in shrublands (mainly in Texas, Nevada, California,

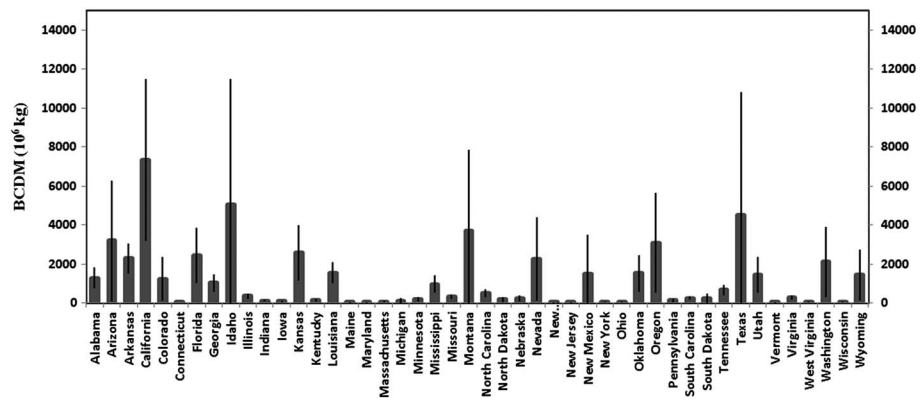


Figure 4. Mean and standard deviation of BCDM from 1995 to 2011 for individual states across the CONUS.

Idaho, and Arizona), 7.7% in grasslands (mainly in Kansas, Texas, Florida, California, and Montana), and 14.1% in croplands (mainly in Arkansas, Texas, Kansas, Florida, and Montana).

The interannual variation in overall biomass consumed presents an increasing trend across the CONUS (Figure 5). The annual CONUS BCDM increased significantly at a rate of 2.87 Tg/yr ( $P$  value = 0.035). For the five CONUS ecosystem types the increase rate was 1.47 Tg/yr ( $P$  value = 0.089) in forest, 0.52 Tg/yr ( $P$  value = 0.003) in savanna, 1.48 Tg/yr ( $P$  value = 0.016) in shrubland, 0.36 Tg/yr ( $P$  value = 0.007) in grassland, and 0.42 Tg/yr ( $P$  value = 0.012) in cropland (Figure 5). During this period, very high BCDM occurred in 2000, 2007, and 2011. The increase of biomass consumed over the CONUS can be mainly attributed to the contribution of only a few states. The states both with a significantly increased trend ( $P$  value < 0.1) and with more than 2% of the total average annual CONUS biomass consumed were New Mexico (0.208 Tg/yr), Oklahoma (0.116 Tg/yr), Florida (0.143 Tg/yr), Arizona (0.399 Tg/yr), Texas (0.679 Tg/yr), and California (0.358 Tg/yr).

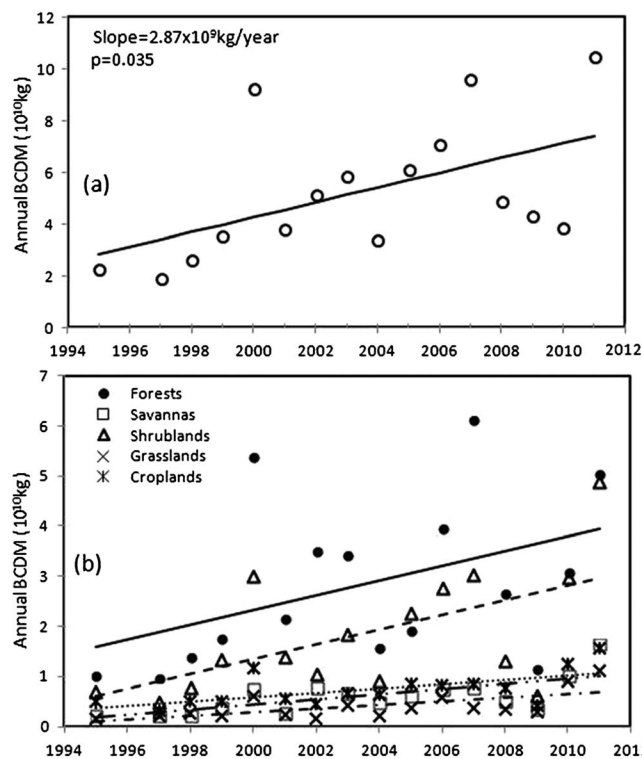
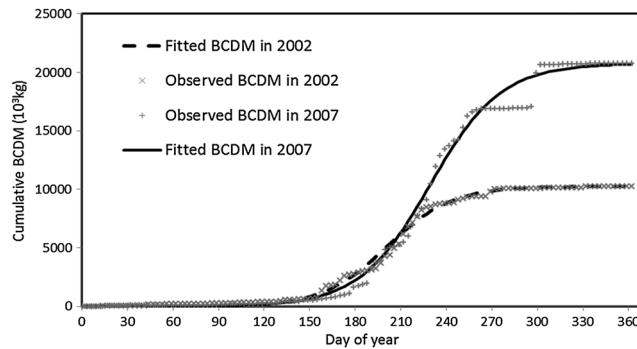


Figure 5. Interannual trend in biomass consumption from 1995 to 2011. (a) Total BCDM across CONUS and (b) BCDM in the five CONUS ecosystems reclassified from GLCC ecosystem types provided in the WF\_ABBA fire product.

### 3.2. Spatial Pattern of Fire Biomass Consumed Seasonality

The seasonality of fire was derived using the sigmoidal function (equation (2)), which describes the cumulative distribution of biomass consumed. In general, the cumulative BCDM exhibits one of two different types of temporal trajectory that are illustrated in Figure 6 for the state of California for 2002 and 2007. The results for 2002 are typical of most states and years where there are no extreme fire events with the cumulative BCDM increasing gradually as more fires occur through the fire season. The results for 2007 show an abrupt increase in the cumulative BCDM because of a very large fire event occurring after several small fire events. These very large fire events result in slightly greater errors in the functionally fitted curve, but their impact is expected to be negligible compared to the general pattern of the temporal BCDM. Moreover, the fitted temporal pattern



**Figure 6.** Examples of fitting temporal trajectories to cumulative BCDM (equation (2)) in California 2002 and 2007 data.

smooths any temporally irregular variation of the estimated daily BCDM. Overall, the sigmoidal function fits daily biomass consumed well, with  $R^2 > 0.95$  and  $P$  value  $< 0.00001$  for the greater majority of years and  $1^\circ$  grid cells.

The start of the fire season (Figure 7a) occurs first (January–February) in the southeast CONUS (particularly, day of year (DOY)  $56 \pm 30$  in Florida) and shifts to later in the spring further northward and westward.

The fire season start is also early (February and March) in some of the South West and Central States (Texas, Oklahoma, and Arkansas). The latest start of the fire season is in June in the northwest CONUS and other states southeast of the Great Lakes. Figure 8a shows the mean start of the fire season for contiguous states from Texas to Washington and indicates a fire season start date difference of 97 days from DOY  $86 \pm 20$  (Texas) to  $184 \pm 24$  (Idaho). Along the east coast, the fire occurrence was limited, except in Florida and Georgia, but the spatial variation of the start of the fire season shifted by 103 days from DOY  $56 \pm 30$  in Florida to DOY  $158 \pm 18$  in Pennsylvania (Figure 8b).

The peak day of biomass burning varies from June to mid-August in the majority of the CONUS (Figure 7b). The peak occurs early (June) in the central parts of the CONUS and some eastern regions and occurs later (end of July to early August) in the northwest. Interestingly, the earliest peak occurs in Florida (in March) while

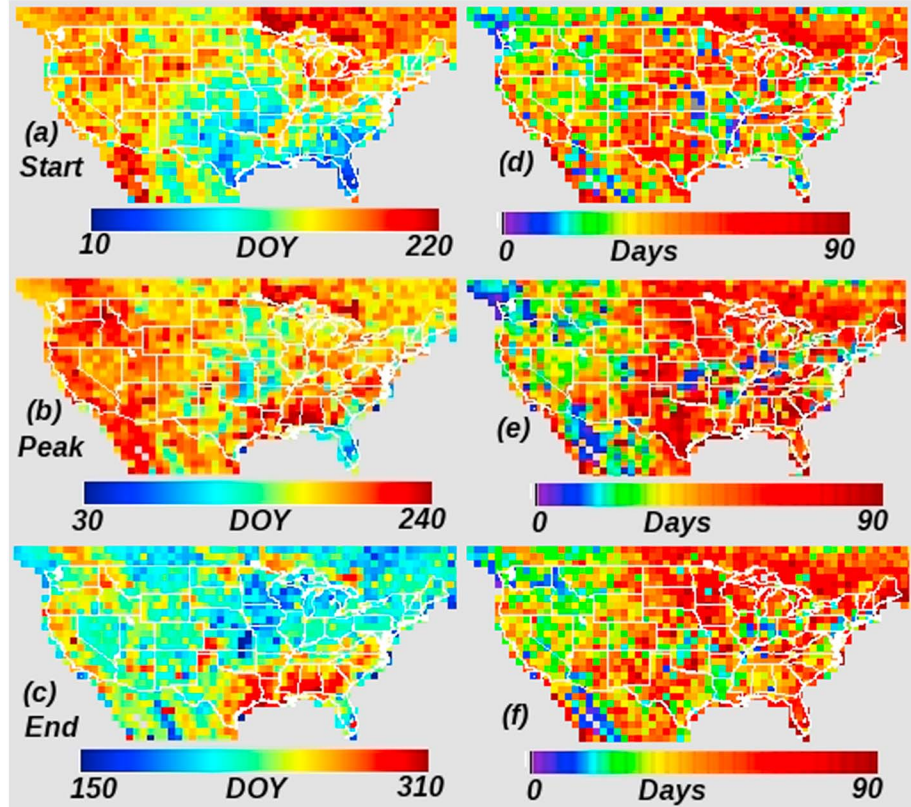


**Figure 7.** (a–c) The 17 year average and (d–f) interannual variation of the fire seasonality metrics defined at a  $1^\circ$  grid. Day of year mean start, peak, and end of the fire season, and corresponding standard deviation start, peak, and end of the fire season. All grid cells had at least one GOES fire detection over the 17 years.



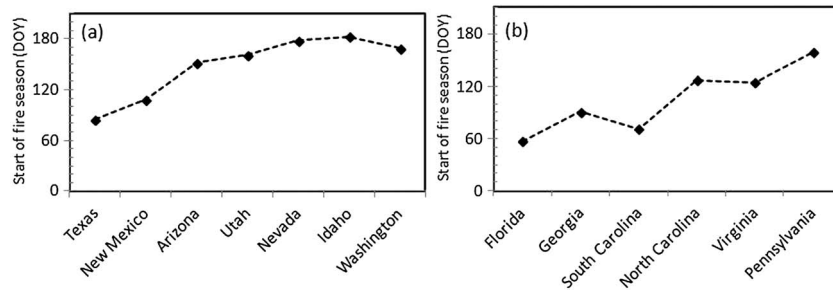


**Figure 8.** Regular spatial shifts (from south to north) in the start of the fire season for states in (a) Middle West and (b) east coast.

the latest peak occurs in Alabama (in September); both are located in the southeastern region. This pattern is perhaps associated with agricultural practices [McCarty, 2011] and dry conditions in Florida (illustrated in section 3.4). It could also be associated with lightning fires that are particularly prevalent in Florida and the Gulf States [Orville et al., 2002; Peterson et al., 2010].

The end of the fire season mainly occurs from August to October (Figures 7c). It arrives late in the southeast CONUS in states such as Alabama, Georgia, and Louisiana, where the fire season ends mid- to late October. In western states, such as Texas, California, and Oregon, the fire season ends at the end of September. In contrast, the fire season ends early in Florida ( $223 \pm 37$ ), Vermont ( $216 \pm 53$ ), and Wisconsin ( $219 \pm 41$ ). It also ends relatively early (August) in the Corn Belt, which is likely to be associated with agricultural practices [Tulbure et al., 2011].

The interannual variation in the start, peak, and end of the fire season (Figures 7d–7f) is for most regions quite high. The illustrated standard deviations indicate the following differences: the start of the fire season variation is greater than 1 month for most states and up to 3 months in the central states (Figure 7d), for the peak the variation is less than 1 month in the western CONUS and as large as 3 months in the central and eastern CONUS (Figure 7e), and for the end of the fire season the variation is less than 1 month in western and southeastern CONUS and again up to 3 months in the central states (Figure 7f).

Considering individual states, the duration of the fire season varies from 2 to 6 months (Figure 9). Although the biomass consumed is greatest in the western and mountain states of Idaho, Montana, Oregon, Arizona, and California, the corresponding fire season durations are less than 3.5 months. In contrast, the fire season is longest in the south and southeast, including in Oklahoma, Florida, Louisiana, Alabama, South Carolina, and Georgia, where the fire season lasts as long as 6 months. For most states, the fire season duration varies among years and differs by less than 1 month, but the difference can be as

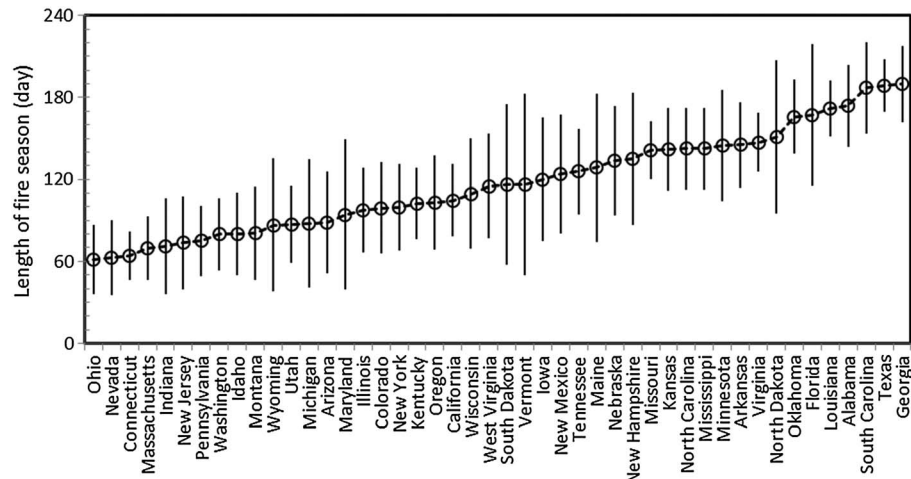


**Figure 9.** Mean 17 year fire season duration (circles) and standard deviations (vertical lines) for all the CONUS states.

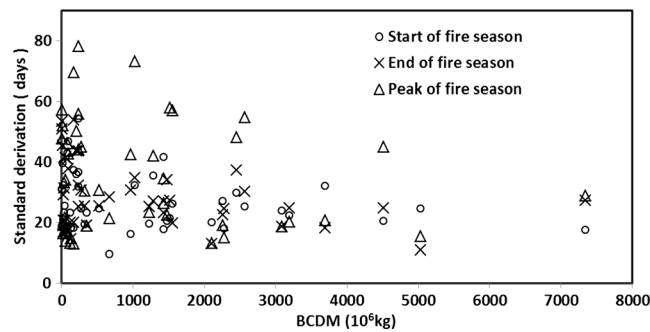


**Figure 10.** Relationship between the standard deviation of the state mean fire seasonality (start, peak, and end metrics) with the state mean annual BCDM. Results computed at the state level (symbols) with respect to the 17 years of data.

great as 2 months in some regions such as Vermont and South Dakota. At the state level, the interannual variation of the start, peak, and end of the fire season, particularly the peak, is negatively correlated to the 17 year average annual biomass consumed (Figure 10). In other words, the fire season metrics show small interannual variation in the states where biomass burning occurs frequently. This is likely because fire occurrences are episodic events which are randomly distributed within a potential fire season.

### 3.3. Interannual Trend in Fire Biomass Consumed Seasonality

In general, the fire seasonality metrics have significant interannual trend in several states but significant trends were not evident over the entire CONUS. Below only those states with significant trends ( $P$  value  $< 0.1$ ) for the start, end, and duration of the fire season, respectively, are discussed. A significant trend for an earlier start of the fire season (1.5–5 d/yr) occurred for Alabama, Arkansas, Georgia, Iowa, Kansas, Louisiana, Mississippi, Ohio, Oklahoma, South Carolina, Texas, Virginia, and Wisconsin. In contrast, a significant trend for a later start of the fire season occurred for Arizona (2.1 d/yr) and Oregon (2.2 d/yr).

The end of the fire season tended to shift to an earlier date in several states. A significant trend occurred for Alabama, California, Colorado, Florida, Georgia, Kansas, Kentucky, Louisiana, Maine, Maryland, Mississippi, Missouri, North Carolina, North Dakota, Nebraska, South Carolina, Tennessee, Texas, Virginia, and West Virginia. The rate of shift was 1.5–5 d/yr, which is similar to the start of the fire season shifts.

The fire season duration only showed significant trends in eight states. They were Alabama, Arizona, California, Colorado, Louisiana, Maryland, Minnesota, and Tennessee. Among these, the fire season duration reduced in Arizona (4.0 d/yr,  $P$  value = 0.039), California (2.5 d/yr,  $P$  value = 0.066), and Colorado (3.6 d/yr,  $P$  value = 0.04), with the biomass consumed being largest in California and fifth largest in Arizona.

### 3.4. Variation in Biomass Consumed Seasonality With Climate Changes

The spatial distribution of the fire seasonality in this study shows that high seasonal temperatures lead to an earlier start and later end to fires (Figures 7 and 8). In the Middle West, the spatial shift in the start of the fire season certainly follows the warm spring temperature, which arrives early in Texas and late in Idaho. This is also apparent in the eastern region from Florida to Pennsylvania. The shift of timing spans about 4 months from the end of February (Florida) to the end of June (Idaho) for the start of the fire season and 3 months from early August (Vermont) to late October (Alabama) for the end of the fire season. This latitudinal gradient is associated with the northward (in spring) and southward (in autumn) progress of temperature. However, a regular pattern of spatial shifts in all the fire season metrics across the entire CONUS is not evident. Clearly, the spatial pattern of the fire seasonality is more complex than the seasonal variation in temperature because factors including the precipitation (fuel moisture), fuel abundance and spatial structure, and sources of fire ignition may also play significant roles [Morgan et al., 2008; Archibald et al., 2009; van der Werf et al., 2008; Westerling et al., 2011].

Climate change has evident significant impacts on the interannual variation in the fire seasonality in some states. The start of the biomass burning season is negatively correlated with anticipated and current temperature at state scales. It is found that the interannual temperature variation has a significant influence on the start of the fire season in Maine, North Dakota, Oregon, Nevada, Pennsylvania, Ohio, Illinois, Indiana, Virginia, Kentucky, Tennessee, Texas, Arkansas, Mississippi, and Louisiana. For example, the start of the fire season in Oregon, where BCDM accounts for 6% over the CONUS, has been delayed 2.2 d/yr ( $P$  value = 0.079) and appears to be related to the decrease in temperature from spring to early summer (Figure 11). The annual time series in Oregon indicates that relatively high temperatures in March–April induce early fire

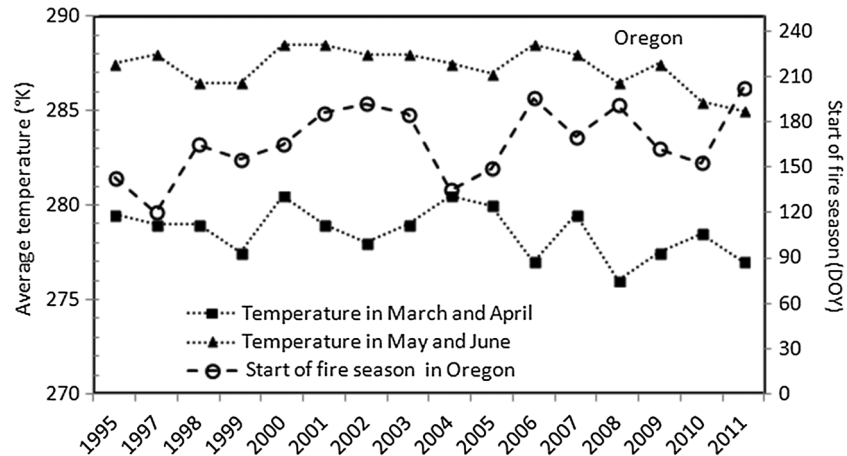


**Figure 11.** Annual variation in the start of the fire season with the spring (March and April) and early summer (May and June) mean temperature in Oregon. For reference, the day of the year (DOY) for 1 April and 1 June are 91 and 152, respectively.

occurrences, such as in 2004, 2007, and 2010, while low spring temperatures delay the fire season occurrence, such as in 2002, 2006, 2008, and 2011.

Interannual variation in the end of the fire season is also influenced by antecedent temperature. A significant correlation is found in the states of Washington, Montana, North Dakota, Wisconsin, South Dakota, Nevada, Iowa, Utah, Nebraska, Illinois, Arizona, Arkansas, and Alabama. In Arizona, for example, the end of the fire season is significantly associated with temperature change in September ( $P$  value = 0.057) (Figure 12), which is prior to the end of the fire season. In other words, the fire season tends to end early with a low temperature in September in Arizona.

High precipitation is generally associated with a delay in the start of the fire season and a later end of the fire season. The start of the fire season was significantly correlated with precipitation in the current and previous month for Minnesota, South Dakota, Iowa, Illinois, Missouri, Tennessee, Arkansas, South Carolina, Louisiana, Georgia, and Florida. Detailed correlations for Florida and Georgia, where biomass burning emissions are the greatest in the eastern region, are illustrated in Figure 13. Generally, in Florida, an early start to the fire season corresponds to dry conditions in January and February, so that the start of the fire season is significantly correlated to precipitation in January and February ( $P$  value < 0.08). In Georgia, the start of the fire season has similar variation with monthly precipitation. Spring precipitation was high before 1999, which seems to have resulted in the start of the fire season occurring later in May, whereas after 2001 early spring (January and February) was relatively dry and the fire season started earlier in February and March. Further examination indicates that the fire season presents a trend to an earlier start (5.5 d/yr,  $P$  value < 0.005) in response to a significant precipitation (January–March) reduction trend ( $P$  value < 0.05) (Figure 13b). The end

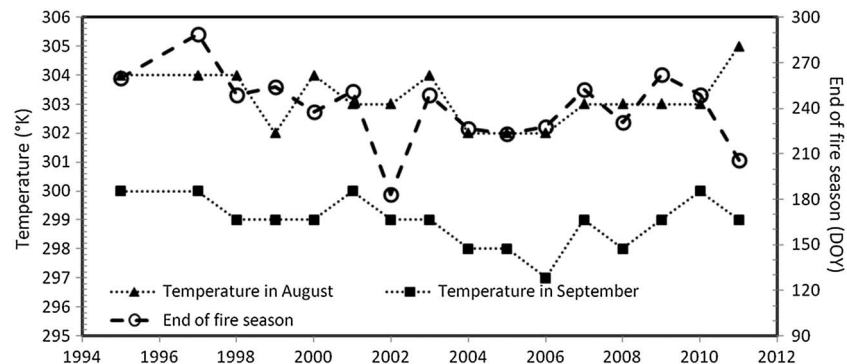


**Figure 12.** Annual variation in the end of the fire season with the mean August and September temperatures in Arizona. For reference, the day of the year (DOY) for 1 September is 213.

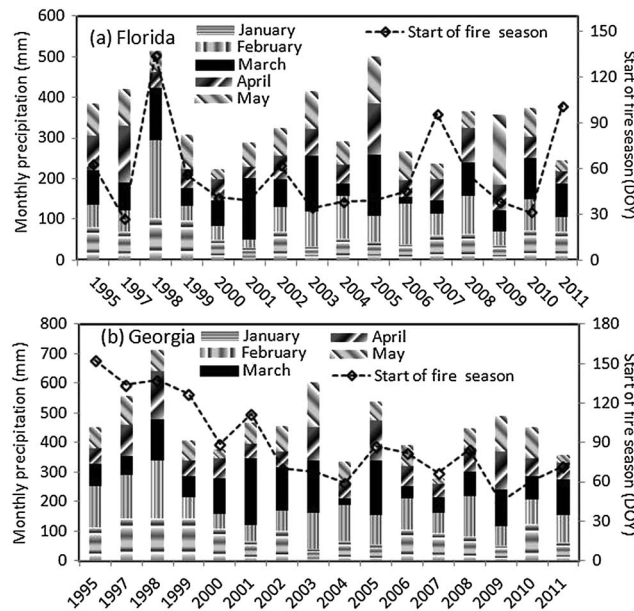


**Figure 13.** Annual variation in the mean state January to May precipitation (bars) with the start of the fire season (dashed line) in (a) Florida and (b) Georgia.

of the fire season was significantly correlated with precipitation in Washington, Idaho, Vermont, Wisconsin, California, Utah, Indiana, Missouri, Georgia, Alabama, and Mississippi.

The fire seasonality and the degree of biomass consumption are expected to be impacted by drought. Our analysis indicates that both the start and end of the fire season have a generally poor correlation with the PDSI in the current and previous month. A significant correlation between the PDSI and the start of the fire season occurred for Washington, Minnesota, North Dakota, Tennessee, South Carolina, Mississippi, Louisiana, and Florida, while a significant correlation for the end of the fire season occurred for Idaho, Minnesota, Oregon, Wyoming, Illinois, Colorado, Texas, Arkansas, and Florida. The correlations were positive or negative, which implies more complexity than the simple

assumption that the fire season occurs earlier and ends later in accordance with the PDSI-derived severe or extreme drought score. By contrast, the 17 annual BCDM estimates compared with the mean state PDSI had significant exponential relationships (Figure 14) for 19 states which are Washington, Maine, Oregon, New York, California, Utah, Ohio, Illinois, Indiana, Colorado, West Virginia, Kentucky, New Mexico, Tennessee, Texas, Georgia, Mississippi, Louisiana, and Florida. These PDSI results should be treated with caution as the PDSI may not identify droughts on timescales shorter than 12 months when monthly PDSI values are used [Vicente-Serrano *et al.*, 2010]. However, our result suggests that the PDSI is an effective index for reflecting the interannual variation of total biomass consumed.

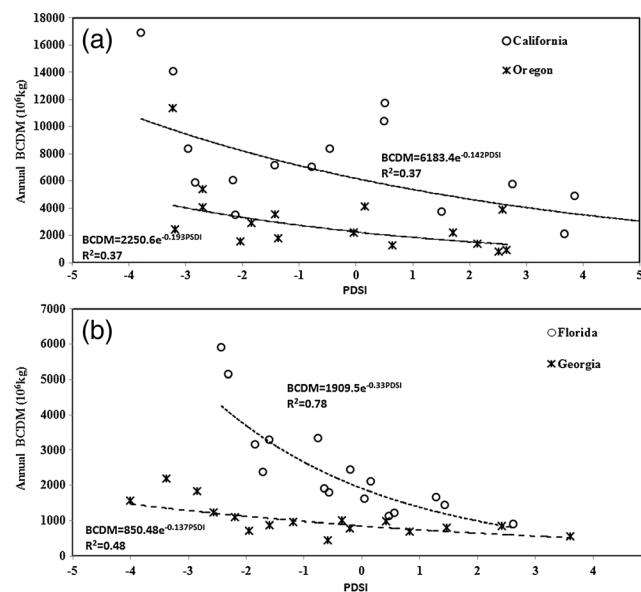


**Figure 14.** Relationship between the state mean annual BCDM and the state mean Palmer drought index (PDSI) for (a) two western states and (b) two southeast states for the 17 years of data.

## 4. Discussion

### 4.1. Uncertainty of Biomass Burning Estimates

This study has focused on the interannual and seasonal variations in BCDM. Therefore, any systematic uncertainties in the BCDM will have limited impact. The uncertainty in the BCDM mainly comes from the GOES FRP data and the underlying assumptions implicit in the conversion of FRP to BCDM. It is established that the calculation of biomass consumed from FRP data is sensitive to the satellite sampling, as fires may not be burning at the time of satellite observation, or may be sensed when the fire is not fully burning, and because the fire behavior can fluctuate rapidly in space and time [Smith and Wooster, 2005; Kumar *et al.*, 2011; Boschetti and Roy, 2009]. However,

these factors likely have limited impacts on the state level fire seasonality and interannual variation because they mainly occur randomly in any annual period. However, FRP sampling issues associated with clouds and satellite active fire detection capabilities may introduce more systematic biases and are discussed below.

Satellite FRP is only computed when there is an active fire detection. Active fire detection is precluded, however, when fires are obstructed by cloud cover, optically thick smoke, and perhaps by overstory vegetation for certain surface fires [Giglio *et al.*, 2003; Roy *et al.*, 2008]. By analyzing precipitation, fire history, and cloud mask data, GOES active fire detection omission errors over the Brazilian Amazon were quantified as 11% [Schroeder *et al.*, 2008]. As most of the CONUS is not more cloudy than the Brazilian Amazon, it is reasonable to assume a similar level of GOES active fire detection omission error for this study. The methodology to model the diurnal variation in FRP data at individual fire pixel locations (section 2.1) largely negates the impact of transient clouds. However, if clouds persist for the duration of the fire, then there is no FRP data to reliably model from. The incidence of this issue is not possible to quantify. If we assume that the occurrence of cloud obscuration is random with respect to fire time and duration, then cloud impacts on the results of this study can be ignored. If the degree of persistence of cloudiness over the duration of fires changed in some systematic manner over the 17 years of the study, then a systematic temporal bias would be introduced. However, time series of seasonal anomalies of total cloud cover present no trend over the CONUS for this study period [Warren *et al.*, 2007].

Only actively flaming or smoldering fires that are sufficiently large and/or hot to be detected will have associated FRP data [Prins and Menzel, 1992; Giglio *et al.*, 2003; Roberts *et al.*, 2005; Zhang *et al.*, 2011]. For these reasons, it is established that geostationary satellite data may have significant active fire omission errors [Roberts and Wooster, 2008]. The GOES satellite viewing geometry varies in a temporally fixed manner with pixel sizes varying from 4 to 10 km across the CONUS. Consequently, the northwestern CONUS, which is observed with the highest GOES view zenith angles, has reduced likelihood of active fire detection due to the coarser spatial resolution. Comparison of Landsat-mapped burned areas with GOES active fire detections indicated that the GOES imager detects about 40% of small fires ( $<1 \text{ km}^2$ ) and more than 80% of large fires ( $>10 \text{ km}^2$ ) across the CONUS [Zhang *et al.*, 2011]. The large number of undetected small fires accounts for a burned area of less than 5% and the small number of large cool fires that were undetected could contribute more error, which together lead to an estimated GOES detection error across the CONUS of less than 15% [Zhang *et al.*, 2011]. Fundamentally, any contribution from small and cool fires that are undetected by GOES will not be considered in this study, and therefore, any trends in small and cool fire BCDM are unexamined by this study.

This paper is concerned with BCDM. Following standard convention, and as discussed in section 2.1, we assumed that the biomass combustion rate ( $\beta$ ) used in equation (1) was constant. The impact of fuel dryness on the biomass combustion rate has not been well quantified in satellite-based FRE studies. A recent laboratory study indicated that fuel moisture could cause an uncertainty of as much as 11% in the biomass combustion rate [Smith *et al.*, 2013]. However, because fuel is generally dried before burning, we assume a constant combustion rate, as have other researchers [e.g., Ellicott *et al.*, 2009; Roberts *et al.*, 2009; Kaiser *et al.*, 2012].

#### 4.2. Independent Comparison With Other Biomass Consumed Data Sets

There is no reliable way to validate biomass consumed data sets at landscape scale, because validation of BCDM requires accurate measurements of biomass consumed in fire events, which are currently unavailable over large areas and are too expensive and time-consuming to obtain. Instead, to further verify the quality of the BCDM estimates, they were compared with other similar data sets that are also not validated.

First, the daily CONUS biomass consumed estimates for 2010 were compared with estimates derived using the MODIS vegetation property-based fuel system and burned area estimated from subpixel fire size in the GOES WF\_ABBA fire product [Zhang *et al.*, 2008]. The daily total estimates in these two data sets were comparable with a relative difference of 5.7%, and a strongly significant linear relationship ( $R^2 = 0.88$ ) with a slope of  $0.968 \pm 0.019$  [Zhang *et al.*, 2012]. Because the fire sources in these two estimates were all from GOES, the comparison only verifies that the FRE is an effective proxy to replace burned area and fuel loading for the estimates of biomass burning from wildfires.



Second, the CONUS annual biomass consumed estimates were compared with biomass consumed defined by the Global Fire Emissions Database (GFED3.1) [van der Werf *et al.*, 2010] for 1997 to 2010. GFED biomass consumed estimates are derived from model outputs and calibrated MODIS fire products and do not use FRP data. Comparison results show that the estimates of annual biomass consumed during the 14 years correlate with the GFED estimates well ( $P < 0.001$ ) but are larger than GFED by a factor of 1.2 to 3.3. We note that GFED emissions are thought to be underestimated over the CONUS [Al-Saadi *et al.*, 2008; Kaiser *et al.*, 2012].

Third, the annual biomass burning estimates were compared with three forest biomass consumption estimates derived for the western CONUS for 2002 to 2006 by Ghimire *et al.* [2012]. These estimates were 6.88 TgC/yr (based on forest inventory data, tree mortality, and burned severity from Monitoring Trends in Burn Severity (MTBS) where only large fires ( $>4 \text{ km}^2$ ) were included), 29 TgC/yr (derived from MODIS active fires and land cover-based fuel loading), and 7 TgC/yr (derived from MTBS burned area and Fuel Characteristics Classification System fuel loading (Wildland Fire Emissions Information System, <http://wfeis.mtri.org/>)). The biomass burning calculated in our study for the forest ecosystem over the western CONUS for 2002 to 2006 was 10.4 TgC/yr derived from the mean annual BCDM estimates by assuming a 0.45 dry biomass carbon proportion [Schlesinger, 1991]. This value is within the range of the three estimates reported by Ghimire *et al.* [2012].

### 4.3. Impacts of Human Activity on Biomass Burning and Seasonality

Human pyrogenic activities have also altered the variation in the fire seasonality across CONUS and are thought to be due to land use practices, primarily agriculture [McCarty, 2011; Tulbure *et al.*, 2011]. These synoptic studies of agricultural burning have been driven by satellite data; however, satellite mapping of agricultural fires is known to be challenging [Roy *et al.*, 2008]. Biomass burning in cropland is related to field-clearing practices and to crop harvest. In the Corn Belt, winter wheat (October to April) is harvested and burned in April and May before the next planting of corn or soybean [Le Page *et al.*, 2010b]. This timing matches well with the start of biomass burning occurrences detected from BCDM in this study.

The long-term BCDM seasonality reveals an early shift trend in the central CONUS where agricultural lands are dominant. This shift has occurred at both the start and the end of biomass burning season, which leads to no significant trend in the fire season duration. This early shift is likely to be attributed to changes in human agricultural practices: in order to increase crop yield by lengthening grain fill periods, there has been a trend to earlier planting dates [Kucharik, 2006; Conley and Santini, 2007]; accordingly, corn and soybean planting dates have advanced by 0.4 and 0.49 d/yr, respectively, from 1981 to 2005, and both crop types have experienced a trend to earlier harvest dates [Sacks and Kucharik, 2011]. This trend in crop practice illustrates the early shift of the fire seasonality well, although the shift rate in crop season is smaller than the shift of the fire season. In much of the CONUS, a biannual rotation between corn and soybeans is common but multiple crops rotated over several years can also occur [Plourde *et al.*, 2013]. It should be noted that our approach, which detects only the start of the first season and the end of last fire season during a year within a grid cell of state, will not detect multiple fire cycles that may occur. If the number of fire cycles varies interannually, such as where fires are related to crop rotation, the detected fire seasonality would present a large variability.

## 5. Conclusions

Long-term biomass burning derived from geostationary satellite data was used to investigate the interannual variation in biomass consumed and the fire seasonality. The results show that biomass consumed across the CONUS significantly increased at a rate of 2.87 Tg/yr, while there is considerable interannual variation. The increased rate is largest for forests, followed by shrubland, savannas, croplands, and grasslands. However, the seasonal length of biomass burning has revealed no significant change, except for a shortening trend in several states over the western CONUS. This suggests that the frequency of extreme fire events could increase with the increase in extreme weather conditions [IPCC, 2012], such as summer drought extremes and the duration of these droughts.

The spatial pattern of the fire season shows pronounced variability. The timing spans about 4 months from the end of February (Florida) to the end of June (Idaho) for the start of the fire season, 5 months from early April (Florida) to mid-September (Alabama) for the peak season, and 3 months from early August (Vermont) to the end of October (Alabama) for the end of the fire season. Although the spatial pattern of the

fire season is complex because it is controlled by numerous factors across the CONUS, it appears to shift regularly in various local regions in response to the latitudinal gradient of temperature variation.

The fire seasonality presents considerable interannual variation and significant trends in the start and end of the fire season occur in various states. The preliminary results of this study indicate that the trends are more strongly associated with temperature in the west and with precipitation in the southeast. Literature review suggests that agricultural practices may explain fire seasonality changes, particularly in the central CONUS. While the PDSI was found to have been an effective index reflecting interannual variation in the total biomass consumed, it had limited correlation with the fire seasonality. Importantly, the reported state level correlations between the fire season metrics and antecedent monthly temperature and precipitation simply demonstrate potential climate influences. Independent examination of these factors provides useful insights but we recognize that these and other multiple factors may combine in complex ways. The correlations are only significant in some states because other factors may dominate. The temporal and spatial pattern of biomass consumed from wildfires is the final consequence of a sequence of influences from climate, fuel loadings, land cover and land use, and lightning and anthropogenic sources of ignitions, which are complex to disaggregate.

The frequency and seasonality of fire have conventionally been derived by examination of summary statistics of satellite-derived burned area maps or active fire counts. In this study the biomass consumed derived from geostationary satellite data are reported and so are not expected to reveal the same patterns as conventional approaches. The use of biomass consumed estimates is more directly appropriate to studies of biomass burning emissions, including carbon and aerosol amounts, as it is well established that emissions are dependent on the fuel condition and the fire behavior which are not reliably defined using conventional remote sensing techniques but are captured by the temporal integration of geostationary FRP. Further research to compare the fire seasonality derived using the reported approach with more conventional approaches is recommended.

#### Acknowledgments

We wish to thank Christopher Schmidt for providing GOES WF\_ABBA V65 fire data. The views, opinions, and findings contained in these works are those of the author(s) and should not be interpreted as an official NOAA or U.S. government position, policy, or decision. We thank the reviewers whose comments helped us to improve this manuscript.

#### References

- Al-Saadi, J., et al. (2008), Evaluation of near-real-time biomass burning emissions estimates constrained by satellite active fire detections, *J. Appl. Rem. Sens.*, *2*, doi:10.1117/1.2948785.
- Archibald, S., D. P. Roy, B. W. Van Wilgen, and R. J. Scholes (2009), What limits fire?: An examination of drivers of burnt area in sub-equatorial Africa, *Global Change Biol.*, *15*, 613–630, doi:10.1111/j.1365-2486.2008.01754.x.
- Balshi M. S., et al. (2007), The role of historical fire disturbance in the carbon dynamics of the panboreal region: A process-based analysis, *J. Geophys. Res.*, *112*, G02029, doi:10.1029/2006JG000380.
- Balshi, M. S., A. D. Mcguire, P. D. Ffy, M. Flannigan, J. Walsh, and J. Melillo (2009), Assessing the response of area burned to changing climate in western boreal North America using a Multivariate Adaptive Regression Splines (MARS) approach, *Global Change Biol.*, *15*, 578–600, doi:10.1111/j.1365-2486.2008.01679.x.
- Bond, W. J., and J. E. Keeley (2005), Fire as a global 'herbivore': The ecology and evolution of flammable ecosystems, *Trends Ecol. Evol.*, *20*, 387–394, doi:10.1016/j.tree.2005.04.025.
- Boschetti, L., and D. P. Roy (2009), Strategies for the fusion of satellite fire radiative power with burned area data for fire radiative energy derivation, *J. Geophys. Res.*, *114*, D20302, doi:10.1029/2008jd011645
- Bowman, D., et al. (2009), Fire in the Earth system, *Science*, doi:10.1126/science.1163886.
- Burgan, R. E., R. W. Klaver, and J. M. Klaver (1998), Fuel models and fire potential from satellite and surface observations, *Int. J. Wildland Fire*, *8*, 159–170.
- Chandler, C., P. Cheney, P. Thomas, L. Trabaud, and D. Williams (1983), *Fire in Forestry Vol. 1: Forest Fire Behavior and Effects*, John Wiley, New York.
- Chapin, F. S., T. S. Rupp, A. M. Starfield, L. DeWilde, E. S. Zavaleta, N. Fresco, and A. D. McGuire (2003), Planning for resilience: Modeling change in human-fire interactions in the Alaskan boreal forest, *Front. Ecol. Environ.*, *1*, 255–261.
- Chapin, F. S., P. A. Matson, and H. A. Mooney (2002), *Principles of Terrestrial Ecosystem Ecology*, Springer, New York.
- Chen, Y., J. T. Randerson, D. C. Morton, R. S. DeFries, G. J. Collatz, P. S. Kasibhatla, L. Giglio, Y. Jin, and M. E. Marlier (2011), Forecasting fire season severity in South America using sea surface temperature anomalies, *Science*, *334*, 787–791.
- Chuvieco, E., L. Giglio, and C. Justice (2008), Global characterization of fire activity: Toward defining fire regimes from Earth observation data, *Global Change Biol.*, *14*, 1488–1502, doi:10.1111/j.1365-2486.2008.01585.x.
- Conley, S. P., and J. B. Santini (2007), Crop management practices in Indiana soybean production systems, *Crop Manag.*, doi:10.1094/CM-2007-0104-01-RS.
- Csiszar, I., L. Denis, L. Giglio, C. O. Justice, and J. Hewson (2005), Global fire activity from two years of MODIS data, *Int. J. Wildland Fire*, *14*, 117–130, doi:10.1071/Wf03078.
- Dai, A. (2011), Characteristics and trends in various forms of the Palmer Drought Severity Index during 1900–2008, *J. Geophys. Res.*, *116*, D12115, doi:10.1029/2010JD015541.
- Ellicott, E., E. Vermote, L. Giglio, and G. Roberts (2009), Estimating biomass consumed from fire using MODIS FRE, *Geophys. Res. Lett.*, *36*, L13401, doi:10.1029/2009GL038581.
- Flannigan, M. D., B. J. Stocks, and B. M. Wotton (2000), Climate change and forest fires, *Sci. Total Environ.*, *262*, 221–229.
- Freeborn, P. H., M. J. Wooster, W. M. Hao, C. A. Ryan, B. L. Nordgren, S. P. Baker, and C. Ichoku (2008), Relationships between energy release, fuel mass loss, and trace gas and aerosol emissions during laboratory biomass fires, *J. Geophys. Res.*, *113*, D01301, doi:10.1029/2007JD008679.

- Ge, C., J. Wang, and J. S. Reid (2013), Mesoscale modeling of smoke transport over the Southeast Asian Maritime Continent: Coupling of smoke direct radiative feedbacks below and above the low-level clouds, *Atmos. Chem. Phys. Discuss.*, *13*, 15,443–15,492, doi:10.5194/acpd-13-15443-2013.
- Ghimire, B., C. A. Williams, G. J. Collatz, and M. Vanderhoof (2012), Fire-induced carbon emissions and regrowth uptake in western U.S. forests: Documenting variation across forest types, fire severity, and climate regions, *J. Geophys. Res.*, *117*, G03036, doi:10.1029/2011JG001935.
- Giglio, L., I. Csizsar, and C. O. Justice (2006), Global distribution and seasonality of active fires as observed with the Terra and Aqua Moderate Resolution Imaging Spectroradiometer (MODIS) Sensors, *J. Geophys. Res.*, *111*, G02016, doi:10.1029/2005JG000142.
- Giglio, L., J. Descloitres, C. O. Justice, and Y. J. Kaufman (2003), An enhanced contextual fire detection algorithm for MODIS, *Remote Sens. Environ.*, *87*, 273–282.
- Gill, A. M. (1975), Fire and the Australian flora: A review, *Aust. Forest.*, *38*, 4–25.
- Huesca, M., J. Litago, A. Palacios-Orueta, F. Montes, A. Sebastián-López, and P. Escribano (2009), Assessment of forest fire seasonality using MODIS fire potential: A time series approach, *Agric. For. Meteorol.*, *149*, 1946–1955.
- Intergovernmental Panel on Climate Change (IPCC) (2007), Contribution of working group II to the fourth assessment report of the Intergovernmental Panel on Climate Change, in *Climate Change 2007: Impacts, Adaptation, and Vulnerability*, edited by M. L. Parry et al., 976 pp., Cambridge Univ. Press, Cambridge.
- Intergovernmental Panel on Climate Change (IPCC) (2012), A special report of working groups I and II of the Intergovernmental Panel on Climate Change, in *Managing the Risks of Extreme Events and Disasters to Advance Climate Change Adaptation*, edited by C. B. Field et al., 582 pp., Cambridge Univ. Press, Cambridge, U. K., and New York.
- Kaiser, J. W., et al. (2012), Biomass burning emissions estimated with a global fire assimilation system based on observed fire radiative power, *Biogeosciences*, *9*, 527–554, doi:10.5194/bg-9-527-2012.
- Kaiser, J. W., J. Flemming, M. G. Schultz, M. Suttie, and M. J. Wooste (2009), The MACC Global Fire Assimilation System: First emission products (GFASv0), *ECMWF Technical Memoranda*, No. 596, pp. 1–16.
- Kasischke, E. S., N. L. Christensen Jr., and B. J. Stocks (1995), Fire, global warming, and the carbon balance of boreal forests, *Ecol. Appl.*, *5*(2), 437–451, doi:10.2307/1942034.
- Kucharik, C. J. (2006), A multidecadal trend of earlier corn planting in the central USA, *Agron. J.*, *98*, 1544–1550.
- Kumar, S. S., D. P. Roy, L. Boschetti, and R. Kremens (2011), Exploiting the power law distribution properties of satellite fire radiative power retrievals - A method to estimate fire radiative energy and biomass burned from sparse satellite observations, *J. Geophys. Res.*, *116*, D19303, doi:10.1029/2011JD015676.
- Le Page, Y., D. Oom, J. M. N. Silva, P. Jönsson, and J. M. C. Pereira (2010a), Seasonality of vegetation fires as modified by human action: Observing the deviation from eco-climatic fire regimes, *Global Ecol. Biogeogr.*, *19*, 575–588.
- Le Page, Y., G. R. van der Werf, D. C. Morton, and J. M. C. Pereira (2010b), Modeling fire-driven deforestation potential in Amazonia under current and projected climate conditions, *J. Geophys. Res.*, *115*, G03012, doi:10.1029/2009JG001190, ISSN0148-0227.
- Lee, B., P. S. Park, and J. Chung (2006), Temporal and spatial characteristics of forest fire in South Korea between 1970 and 2003, *Int. J. Wildland Fire*, *15*, 389–396.
- Littell, J. S., D. Mckenzie, D. L. Peterson, and A. L. Westerling (2009), Climate and wildfire area burned in western U.S. ecoregions, 1916–2003, *Ecol. Appl.*, *19*(4), 1003–1021.
- Magi, B. I., S. Rabin, E. Shevliakova, and S. Pacala (2012), Separating agricultural and non-agricultural fire seasonality at regional scales, *Biogeosciences*, *9*, 3003–3012, doi:10.5194/bg-9-3003-2012.
- McCarty, J. L. (2011), Remote sensing-based estimates of annual and seasonal emissions from crop residue burning in the contiguous United States, *J. Air Waste Manag. Assoc.*, *61*(1), 22–34, doi:10.3155/1047-3289.61.1.22.
- Mesinger, F., et al. (2006), North American Regional Reanalysis, *Bull. Am. Meteorol. Soc.*, *87*, 343–360.
- Morgan, P., E. K. Heyerdahl, and C. E. Gibson (2008), Multi-season climate synchronized forest fires throughout the 20th century, Northern Rocijes, USA, *Ecology*, *89*(3), 717–728.
- Orville, R. E., G. R. Huffines, W. R. Burrows, R. L. Holle, and K. L. Cummins (2002), The North American Lightning Detection Network (NALDN)—First results: 1998–2000, *Mon. Weather Rev.*, *130*, 2098–2109.
- Palmer, W. C. (1965), Meteorological drought, Rep. 45, 58 pp., U.S. Dept. of Commerce, Washington, D. C. [Available at <http://www.ncdc.noaa.gov/oa/climate/research/drought/palmer.pdf>]
- Pausas, J. G., and J. E. Keeley (2009), A burning story: The role of fire in the history of life, *BioScience*, *59*, 593–601.
- Pereira, M. G., B. D. Malamud, R. M. Trigo, and P. I. Alves (2011), The history and characteristics of the 1980–2005 Portuguese rural fire database, *Nat. Hazards Earth Syst. Sci.*, *11*, 3343–3358, doi:10.5194/nhess-11-3343-2011.
- Peterson, D., E. Hyer, and J. Wang (2013a), A short-term predictor of satellite-observed fire activity in the North American boreal forest: Toward improving the prediction of smoke emissions, *Atmos. Environ.*, *71*, 304–310.
- Peterson, D., J. Wang, C. Ichoku, E. Hyer, and V. Ambrosia (2013b), A sub-pixel-based calculate of fire radiative power from MODIS observations: 1. Algorithm development and validation, *Remote Sens. Environ.*, *129*, 262–279.
- Peterson, D., J. Wang, C. Ichoku, and L. A. Remer (2010), Effects of lightning and other meteorological factors on fire activity in the North American boreal forest: Implications for fire weather forecasting, *Atmos. Chem. Phys.*, *10*, 6873–6888, doi:10.5194/acp-10-6873-2010.
- Plourde, J. D., B. C. Pijanowski, and B. K. Pekin (2013), Evidence for increased monoculture cropping in the Central United States, *Agr. Ecosyst. Environ.*, *165*, 50–59.
- Pooter, H., and R. Villar (1997), The fate of acquired carbon in plants: Chemical composition and construction costs, in *Plant Resource Allocation*, edited by F. Bazzaz and J. Grace, pp. 39–72, SPB Acad., The Hague, Netherlands.
- Press, W. H., S. A. Teukolsky, and W. T. Vetterling (1997), *Numerical Recipes in C – The Art of Scientific Computing*, 2nd ed., pp. 656–688, Cambridge Univ. Press, Cambridge.
- Prins, E. M., J. M. Feltz, W. P. Menzel, and D. E. Ward (1998), An overview of GOES-8 diurnal fire and smoke results for SCAR-B and 1995 fire season in South America, *J. Geophys. Res.*, *103*(D24), 31,821–31,835, doi:10.1029/98JD01720.
- Prins, E. M., and W. P. Menzel (1992), Geostationary satellite detection of biomass burning in South America, *Trans. Geosci. Rem. Sens.*, *13*, 2783–2799.
- Randerson, J. T., et al. (2006), The impact of boreal forest fire on climate warming, *Science*, *314*, 1130–1132.
- Riaño, D., J. A. Moreno Ruiz, D. Isidoro, and S. L. Ustin (2007), Global spatial patterns and temporal trends of burned area between 1981 and 2000 using NOAA-NASA Pathfinder, *Global Change Biol.*, *13*, 40–50.
- Roberts, G., M. J. Wooster, G. L. W. Perry, N. Drake, L.-M. Rebelo, and F. Dipotso (2005), Retrieval of biomass combustion rates and totals from fire radiative power observations: Application to southern Africa using geostationary SEVIRI imagery, *J. Geophys. Res.*, *110*, D21111, doi:10.1029/2005JD006018.

- Roberts, G. J., and M. J. Wooster (2008), Fire detection and fire characterization over Africa using Meteosat SEVIRI, *IEEE Trans. Geosci. Rem. Sens.*, *46*, 1200–1218, doi:10.1109/Tgrs.2008.915751.
- Roberts, G., M. J. Wooster, and E. Lagoudakis (2009), Annual and diurnal African biomass burning temporal dynamics, *Biogeosciences*, *6*, 849–866.
- Roy, D. P., L. Boschetti, and A. M. S. Smith (2013), Satellite remote sensing of fires, chapter 5, in *Fire Phenomena and the Earth System: An Interdisciplinary Guide to Fire Science*, edited by C. M. Belcher and G. Rein, John Wiley, Chichester, England, doi:10.1002/9781118529539.ch5.
- Roy, D. P., L. Boschetti, C. O. Justice, and J. Ju (2008), The collection 5 MODIS burned area product-Global evaluation by comparison with the MODIS active fire product, *Remote Sens. Environ.*, *112*(9), 3690–3707.
- Russell-Smith, J., B. P. Murphy, C. P. Meyer, G. D. Cook, S. Maier, A. C. Edwards, J. Schatz, and P. Brocklehurst (2009), Improving estimates of savanna burning emissions for greenhouse accounting in northern Australia: Limitations, challenges, applications, *Int. J. Wildland Fire*, *18*, 1–18.
- Sacks, W. J., and C. J. Kucharik (2011), Crop management and phenology trends in the U.S. Corn Belt: Impacts on yields, evapotranspiration and energy balance, *Agric. For. Meteorol.*, *151*, 882–894.
- Schlesinger, W. H. (1991), *Biogeochemistry: An Analysis of Global Change*, Academic Press, New York.
- Schroeder, W., I. Csiszar, and J. Morissette (2008), Quantifying the impact of cloud obscuration on remote sensing of active fires in the Brazilian Amazon, *Remote Sens. Environ.*, *112*(2), 456–470.
- Scott, A. C. (2000), The Pre-Quaternary history of fire, *Palaeogeography, Palaeoclimatology, Palaeoecology*, *164*(1–4), 281–329.
- Smith, A. M. S., and M. J. Wooster (2005), Remote classification of head and backfire types from MODIS fire radiative power and smoke plume observations, *Int. J. Wildland Fire*, *14*, 249–254.
- Smith, A. M. S., W. T. Tinkham, D. P. Roy, L. Boschetti, R. L. Kremens, S. S. Kumar, A. Sparks, and M. J. Falkowski (2013), Quantification of fuel moisture effects on biomass consumed derived from fire radiative energy retrievals, *Geophys. Res. Lett.*, *40*, 6298–6302, doi:10.1002/2013GL058232.
- Taylor, A. H., and C. N. Skinner (2003), Spatial and temporal patterns of historic fire regimes and forest structure as a reference for restoration of fire in the Klamath Mountains, *Ecol. Appl.*, *13*, 704–719.
- Thejll, P., and T. Schmih (2005), Limitations on regression analysis due to serially correlated residuals: Application to climate reconstruction from proxies, *J. Geophys. Res.*, *110*, D18103, doi:10.1029/2005JD005895.
- Tulbure, M. G., M. C. Wimberly, D. P. Roy, and G. M. Henebry (2011), Spatial and temporal heterogeneity of agricultural fires in the central United States in relation to land cover and land use, *Landsc. Ecol.*, *26*, 211–224.
- van der Werf, G. R., J. T. Randerson, L. Giglio, G. J. Collatz, M. Mu, P. S. Kasibhatla, D. C. Morton, R. S. DeFries, Y. Jin, and T. T. van Leeuwen (2010), Global fire emissions and the contribution of deforestation, savanna, forest, agricultural, and peat fires (1997–2009), *Atmos. Chem. Phys. Discuss.*, *10*, doi:10.5194/acpd-10-16153-2010.
- van der Werf, G. R., et al. (2008), Climate regulation of fire emissions and deforestation in equatorial Asia, *Proc. Natl. Acad. Sci. U.S.A.*, *105*(51), 20,350–20,355.
- Vicente-Serrano, S. M., S. Begueria, J. I. Lopez-Moreno, M. Angulo, and A. E. Kenawy (2010), A new global 0.5 degrees gridded dataset (1901–2006) of a multiscale drought index: Comparison with current drought index datasets based on the Palmer Drought Severity Index, *J. Hydrometeorol.*, *11*, 1033–1043, doi:10.1175/2010JHM1224.1.
- Warren, S. G., R. M. Eastman, and C. J. Hahn (2007), A survey of changes in cloud cover and cloud types cover land from surface observations, 1971–96, *J. Clim.*, *20*, 717–738.
- Weaver, J. F., D. Lindsey, D. Bikos, C. C. Schmidt, and E. Prins (2004), Fire detection using GOES rapid scan imagery, *Weather Forecasting*, *19*, 496–510.
- Weber, M. G., and M. D. Flannigan (1997), Canadian boreal forest ecosystem structure and function in a changing climate: Impact on fire regimes, *Environ. Rev.*, *5*, 145–166.
- Westerling, A. L., H. G. Hidalgo, D. R. Cayan, and T. W. Swetnam (2006), Warming and earlier spring increase western US forest wildfire Activity, *Science*, *313*, 940–943.
- Westerling, A. L., M. G. Turner, E. A. H. Smithwick, W. H. Rommed, and M. G. Ryane (2011), Continued warming could transform Greater Yellowstone fire regimes by mid-21st century, *Proc. Natl. Acad. Sci. U.S.A.*, *108*(32), 13,165–13,170.
- Whelan, R. J. (1995), *The Ecology of Fire*, Cambridge Univ. Press, Cambridge, U. K.
- Wooster, M. J. (2002), Small-scale experimental testing of fire radiative energy for quantifying mass combusted in natural vegetation fires, *Geophys. Res. Lett.*, *29*(21), 2027, doi:10.1029/2002GL015487.
- Wooster, M. J., B. Zhukov, and D. Oertel (2003), Fire radiative energy for quantitative study of biomass burning: Derivation from the BIRD experimental satellite and comparison to MODIS fire products, *Remote Sens. Environ.*, *86*, 83–107.
- Wooster, M. J., G. Roberts, G. L. W. Perry, and Y. J. Kaufman (2005), Retrieval of biomass combustion rates and totals from fire radiative power observations: FRP derivation and calibration relationships between biomass consumption and fire radiative energy release, *J. Geophys. Res.*, *110*, D24311, doi:10.1029/2005JD006318.
- Zhang, X., S. Kondragunta, and B. Quayle (2011), Estimation of biomass burned areas using multiple-satellite-observed active fires, *IEEE Trans. Geosci. Rem. Sens.*, *49*, 4469–4482, doi:10.1109/TGRS.2011.2149535.
- Zhang, X., S. Kondragunta, J. Ram, C. Schmidt, and H.-C. Huang (2012), Near real time global biomass burning emissions product from geostationary satellite constellation, *J. Geophys. Res.*, *117*, D14201, doi:10.1029/2012JD017459.
- Zhang, X., S. Kondragunta, C. Schmidt, and F. Kogan (2008), Near real time monitoring of biomass burning particulate emissions (PM2.5) across contiguous United States using multiple satellite instruments, *Atmos. Environ.*, *42*, 6959–6972.